J. Biochem. **143,** 803–811 (2008)
doi:10.1093/jb/mvn034

In vitro Formation of a Novel Type of Membrane Vesicles Containing Dpm1p: Putative Transport Vesicles for Lipid Droplets in Budding Yeast

Yuichi Takeda[1,*,†] and Akihiko Nakano[1,2]

[1]Molecular Membrane Biology Laboratory, RIKEN Discovery Research Institute, 2-1 Hirosawa, Wako, Saitama 351-0198 Japan; and [2]Department of Biological Sciences, Graduate School of Science, University of Tokyo, Hongo, Bunkyo-ku, Tokyo 113-0033, Japan

Received January 13, 2008; accepted February 21, 2008; published online March 14, 2008

A novel type of membrane vesicles was formed *in vitro* from microsomes of *Saccharomyces cerevisiae*, which carries Dpm1p, an enzyme involved in dolichol-sugar synthesis, but not a typical secretory cargo. While COPII vesicles formed *in vitro* were sedimentable by centrifugation at 200,000g_{max} for 15 min, the novel vesicles were not. However, they were sedimented by additional centrifugation at the same speed for 1 h. Immunoelectron microscopy showed that the Dpm1p-containing vesicles had small vesicular/saccular structures of around 40–50 nm in diameter. The addition of glycerol-3-phosphate and oleoyl-CoA, substrates for lipid biosynthesis, significantly enhanced the efficiency of vesicle budding in an ATP-dependent fashion. Dpm1p was localized to lipid droplets as well as endoplasmic reticulum. Fluorescence microscopy further showed that Dpm1p-GFP was present in restricted subregions in isolated lipid droplets. The possibility that the vesicles were intermediates from the endoplasmic reticulum to lipid droplets was examined, and their possible role is discussed.

Key words: Dpm1p, Erg6p, lipid droplet, *Saccharomyces cerevisiae*, vesicle transport.

Abbreviations: ER, endoplasmic reticulum; GFP, (enhanced) green fluorescent protein; GMP-PNP, guanylyl imidodiphosphate; HSP, high-speed pellet; HSS, high-speed supernatant; LD(s), lipid droplet(s); MSS, medium-speed supernatant; RFP, (monomeric) red fluorescent protein.

Lipid droplets (LDs), which are commonly found in eukaryotic cells, are composed of triacylglycerol and steryl ester cores surrounded by phospholipid monolayer (*1–5*). LDs have been regarded as a storage compartment for lipids for a long time, but a recent view proposes its functional roles in many cellular processes (*6*). Indeed, a variety of proteins involved in membrane traffic, cell signaling as well as lipid metabolism have been identified in isolated LDs (*7–10*).

LDs are considered to be derived from the endoplasmic reticulum (ER). Formation of mammalian LDs was reported to be regulated by phospholipase D, extracellular signal-regulated kinase 2 and dynein (*11*), but the mechanism of its biogenesis is still poorly understood. One popular model is that neutral lipids accumulate between the leaflets of the ER membrane, and after reaching a critical size, they bud off into the cytoplasm to form LDs (*1*, *2*, *4*).

Vesicular transport plays an essential role in the intracellular transport of proteins and polysaccharides. It also contributes, in part, to the transport of lipids (*12*). The transport from the ER to the Golgi apparatus is carried out by small transport vesicles termed COPII vesicles (*13*). The formation of COPII vesicles requires the small GTPase Sar1p (*14*), Sec23/24p and Sec13/31p complexes (*13*). Cell-free assays for the budding of COPII vesicles have been established using microsomes isolated from *Saccharomyces cerevisiae* cells and purified COPII proteins (*15–19*). In the microsome-based *in vitro* budding assay, we found that a novel type of membrane vesicles was formed independent of COPII proteins. The vesicles contained Dpm1p (dolichol phosphate mannose synthase), not a typical cargo protein in the secretory pathway. In the present paper, we report characterization of the vesicles and discuss their possible role in the biogenesis of LDs.

MATERIALS AND METHODS

Yeast Strains and Plasmids—*Saccharomyces cerevisiae* strains used in this study were wild-type YPH500 [*MATα ura3 lys2 ade2 trp1 his3 leu2*, (*20*)], KUY136 [*MATα erg6Δ::LEU2 ura3 lys2 ade2 trp1 his3 leu2*, (*21*)], BY4743 (*MATa/α ura3/ura3 lys2/LYS2 his3/his3 leu2/leu2 MET15/met15 dpm1Δ::kanMX4/DPM1*, EUROSCARF Y25598) and YTY102 (*MATa ura3 lys2 his3 leu2 dpm1Δ::KanMX1 DPM1-GFP*, in this study).

To create plasmids for expression of proteins fused with enhanced green fluorescence protein (GFP) and

*Present address: Department of Biochemistry, Osaka University Graduate School of Medicine, 5th Floor, Advanced Research Building, Center for Advanced Science and Innovation, Osaka University, 2-1 Yamada-Oka Suita, Osaka 565-0871, Japan
†To whom correspondence should be addressed. Tel: 81-6-6879-4142, Fax: 81-6-6879-4137,
E-mail: y-takeda@biochem.med.osaka-u.ac.jp

monomeric red fluorescence protein (RFP) at the C-terminus, DNA fragments of GFP and RFP with a stop codon were inserted between the *TDH3* promoter and *CMK1* terminator on a single copy plasmid pTU1 with the *URA3* marker (*22*) to yield pKM1 and pKM2, respectively. The *TDH3* promoter in pKM2 was replaced by the *ADH1* promoter to yield pKM2-2. The fragment of RFP was also inserted into a single copy plasmid pMTG200 with the *TRP1* marker (*23*) to yield pKM3. To construct pYTY102 carrying the *DPM1-GFP* under control of the *DPM1* promoter, the fragment was generated by PCR from the genomic DNA of YPH500 and subcloned into pKM1. To construct *ERG6-RFP*, the fragment encoding *ERG6* promoter and the *ERG6* open reading frame was amplified by PCR and subcloned into pKM2-2 and pKM3, to yield the plasmids pYTY103 and pYTY104, respectively.

The YTY102 strain was obtained from the diploid *dpm1Δ*/*DPM1* strain BY4743 harboring pYTY102 by tetrad analysis utilizing 5-fluoro-orotic acid and G418 plates. *DPM1* is an essential gene and the obtained haploid *dpm1Δ* strain expressing *DPM1-GFP* (YTY102) was viable, confirming that the gene product is functional. Incorporation of *ERG6-RFP* into the *erg6Δ* strain (KUY136) rescued growth delay of the strain (data not shown), indicating that the gene product is also functional.

Yeast cells were grown in YPD [1% Bacto yeast extract (Difco Laboratories, Detroit, MI), 2% polypeptone (Nihon Seiyaku, Tokyo) and 2% glucose] or in MCD [0.67% yeast nitrogen base without amino acids, 0.5% casamino acids (Difco Laboratories) and 2% glucose] medium supplemented appropriately.

Antibodies and Chemicals—Rabbit anti-Pma1p antibody was raised against a synthetic peptide corresponding to residues 55–69 of Pma1p with an additional Cys residue at the C-terminus (GVDDEDSDNDGPVAAC). The antigen peptide was conjugated to keyhole limpet hemocyanin, and used to immunize rabbits. The anti-Pma1p antiserum obtained was affinity-purified over the antigen-immobilized column. Rabbit anti-Emp24p antibody was generated as described (*24*). Antibodies directed against Sec22p (*25*), Sec61p (*26*), Sed5p (*27*) and Erg11p (*28*) were described earlier. Polyclonal anti-Tim23p antibody was kindly provided from the Endo laboratory (Nagoya University). Monoclonal anti-HA (12CA5) and anti-myc (9E10) antibodies were purchased from Roche Diagnostics (Basel, Switzerland). Monoclonal anti-Dpm1p and anti-Pho8p antibodies, polyclonal anti-GFP antibody (A-11122), goat anti-mouse IgG-AlexaFluor488 and goat anti-rabbit IgG-AlexaFluor568 were from Molecular Probes (Eugene, OR). Polyclonal anti-human transferrin antibody was from Bethyl Laboratories Inc. (Montgomery, TX), and polyclonal anti-HA (Y-11) antibody was from Santa Cruz Biotechnology, Inc. (Santa Cruz, CA).

Human transferrin was purchased from Sigma-Aldrich (St Louis, MO) and 6 nm colloidal gold-goat anti-rabbit IgG was from Jackson ImmunoResearch Laboratories, Inc. (West Grove, PA).

Membrane Isolation—Microsomes enriched in the ER membranes were prepared from yeast cells that are grown to a mid-to-late log phase as described before (*29*). LDs were isolated from the cells at a late log phase. Spheroplasts were prepared in the same way as in the isolation of microsomes, and then suspended in homogenization buffer containing 0.2 M sorbitol, 1 mM DTT, 2 mM EDTA, 20 mM Hepes–KOH, pH 7.4 and 1 mM PMSF at the final concentration of 0.3 g wet weight of cell per millilitre. Spheroplasts were subjected to 10 strokes in a Dounce homogenizer on ice using a loosely fitting pestle. The homogenate was centrifuged at 5,000g_{max} at 4°C for 5 min. The supernatant was further centrifuged in an RPS40T rotor (Hitachi, Tokyo) at 36,000 rpm. at 4°C for 30 min. The resulting floating layer containing LDs was collected and mixed with the same volume of 20% (w/w) sucrose in Hepes–KOH, pH 7.4. This suspension was placed beneath buffer B88 (0.25 M sorbitol, 150 mM KOAc, 5 mM MgOAc and 20 mM Hepes-KOH, pH 6.8), and centrifuged in the RPS40T rotor at 36,000 rpm. at 4°C for 1 h. The floating layer containing LDs of high purity was collected (the LD fraction). In the preparations from the cells expressing the fluorescent proteins, yeast inhibitor cocktail (Sigma-Aldrich) was included in the buffers after homogenization. The prepared membranes were used for experiments without freezing, or frozen with liquid nitrogen and stored at −80°C until use.

Protein Analysis—Proteins were quantified by the method of Bradford (*30*) and Peterson (*31*), with bovine serum albumin as a standard. The LD fraction was delipidated by the extraction with two volumes of diethyl ether (*32*, *33*), and the protein content was determined by the latter method.

In Vitro Vesicle Budding Assay—*In vitro* vesicle budding reaction was performed using microsomes as described before (*18*). The basal additives to the reaction mixture were purified COPII proteins (Sar1p, Sec23/24p and Sec13/31p), 0.1 mM guanylyl imidodiphosphate (GMP-PNP), ATP and an ATP regeneration system. In most assays, microsomes were washed with 2.5 M urea in buffer B88 twice and further washed with B88 twice at 4°C. Otherwise indicated, the urea-washed microsomes were used for the assays. The scale of the reaction mixture per one assay was changed depending on the experiments (0.1, 0.4 or 1 ml). After a 30 min of incubation at 25°C or 4°C, the vesicles were separated from donor microsomal membranes by centrifugation at 15,000 rpm in a swing-out rotor (TMS-21, TOMY, Tokyo) at 4°C for 7 min. The medium-speed supernatant (MSS) which contains small vesicles was further centrifuged at 200,000g_{max} in a TLA120.2 rotor (Beckman, Fullerton, CA) at 4°C for 15 min to obtain high-speed pellet (HSP) and high-speed supernatant (HSS) fractions. Proteins in MSS and HSS were precipitated with 7% trichloroacetic acid. The fractions were analysed by SDS-PAGE and immunoblotting.

Fractionations of the vesicles by gradient centrifugation were performed and the details of the procedures were described in the figure legends. The centrifugations were performed in a P55ST2 rotor (Hitachi) at 4°C.

Fluorescence Microscopy—The fluorescence due to GFP and RFP in yeast cells was visualized under an IX-81 microscope (Olympus, Tokyo) equipped with a confocal laser scanner unit CSU10 (Yokogawa Electronic, Tokyo).

Excitation was performed with an argon/krypton laser (Melles Griot) at 488 nm for GFP and at 568 nm for RFP simultaneously. Emissions were collected using a 510–560 nm band-pass filter for GFP and a 590–630 nm band-pass filter for RFP. Images were acquired by a high-resolution digital charge-coupled device camera (C4742-95; Hamamatsu Photonics, Hamamatsu) and were processed by the Aquacosmos software (Hamamatsu Photonics).

Dual colour observation of GFP and Nile Red in the cells was performed using an LSM-510 META confocal laser microscope (Carl Zeiss, Jena, Germany) with an argon laser emitting at 488 nm and with a helium/neon laser emitting at 543 nm. GFP and Nile Red signals were collected using a 505–530 nm band-pass filter and a 560 nm long-pass filter, respectively. The condition under which the leakage of Nile Red fluorescence in the green channel was negligible was used for the experiment.

For immunofluorescence microscopy, cells were formaldehyde-fixed and permeabilized as described (*34*). The cells were incubated with primary antibodies in 3% BSA/PBS for 1 h at room temperature, rinsed and then incubated with the secondary antibodies conjugated to AlexaFluor for 1 h at room temperature. The images were acquired by a LSM 5 PASCAL confocal laser microscope (Carl Zeiss) using the same laser and filter settings as the LSM-510.

Microscopic analysis of the isolated LDs was performed with a BX-51 fluorescence microscope (Olympus), and acquired images were processed by Adobe Photoshop 6.0 software. (NL) All microscopic observations were performed at room temperature.

Lipid Analysis—Lipids of microsomes and the LD fraction were extracted according to Folch *et al*. (*35*). The lipids were applied to silica gel 60 plates (Merck, Darmstadt, Germany), and one-dimensional thin-layer chromatogram was developed by the solvent system, light petroleum-diethyl ether-acetic acid (80: 20: 2, v/v/v). Total phospholipids were quantified by the method of Rouser *et al*. (*36*). The spots of ergosterol and ergosteryl esters were scraped off and dissolved in chloroform, and then quantified by measuring absorbance at 275 nm with ergosterol as a standard (*37*).

Immunoelectron Microscopy—Immunoelectron microscopy of vesicles fixed in 4% paraformaldehyde was performed as described elsewhere (*38*), except that the membranes on grids were stained with uranyl acetate/poly-vinyl alcohol (1 : 9, 4% uranyl acetate: 2% poly-vinyl alcohol). The samples were observed under an H-7100 electron microscope (Hitachi).

RESULTS

Discovery of Novel Vesicles Containing Dpm1p Formed In Vitro from Microsomes—Among several cell-free systems to assess formation of ER-derived COPII vesicles, microsome-based assays are useful for investigating requirements on the membrane side. We were trying to examine whether there were any sorting events of several proteins from microsomes. During such an effort, we fortuitously obtained a peculiar finding. Figure 1A shows a result of a budding assay, looking at the recovery of various proteins into the MSS (15,000 rpm) fraction, which normally contains COPII vesicles during incubation with COPII and GMP-PNP. As expected, cargo proteins such as Sec22p and Emp24p were found in the MSS fraction only when COPII was added, while ER resident proteins such as Erg11p and Sec61p were not. To our surprise, two membrane proteins Dpm1p (an ER protein) and Pma1p (a plasma membrane protein) were found in the MSS fraction, not only in the presence of COPII but also in the absence. To follow the behaviours of these proteins in more detail, we tested ATP- and GMP-PNP-dependence in this *in vitro* assay. As shown in Fig. 1B, the recovery of Pma1p in MSS was ATP-dependent but did not require COPII or GMP-PNP. On the other hand, Dpm1p was released into the MSS fraction regardless of the presence or absence of any of these additives. More detailed analysis on the ATP- and temperature-dependence of the recovery of Pma1p and Dpm1p into MSS is shown in Fig. 1C. The release of Pma1p was highest at 2 mM ATP. Dpm1p was released into MSS even in the absence of ATP, but its amount increased when 1 mM or more ATP was present. The recovery of both Pma1p and Dpm1p into MSS was null or fairly low at 4°C. Sec61p was not detected in MSS under the same condition (data not shown).

Since microsomes were washed with 2.5 M urea before the assay, a possibility existed that the urea washing had caused fragmentation of membranes, which contained Pma1p and Dpm1p and were released into MSS. Figure 1D shows the results of the budding assay with and without the urea washing. As known since before, microsomes washed by the buffer only (B88 alone) produce COPII vesicles without the addition of COPII or GMP-PNP, because endogenous COPII components are still associated with microsomes, which are effectively removed by the urea washing. The release of Pma1p and Dpm1p into MSS, which were seen after the urea washing, was higher with the non-urea-washed microsomes (B88 alone). The urea washing would have removed proteins on the membranes for effective vesicle budding. Such leakage was not seen with Sec61p. From this result, it is unlikely that the spontaneous random fragmentation was induced by the urea washing. Because Sec22p, Pma1p and Dpm1p are all transmembrane proteins, there must be membrane-associated mechanisms for their release into MSS.

To understand the nature of the release of these membrane proteins, MSS from the reaction was separated into HSS (200,000g_{max}, 15 min) and HSP, and HSP was further fractionated by discontinuous sucrose gradient centrifugation. As shown in Fig. 1E, Sec22p (COPII vesicles) and Pma1p were recovered into HSP and sedimented at 30–40% and 30–50% sucrose, respectively, but Dpm1p was partitioned into HSS. The difference in COPII/GMP-PNP/ATP-dependence and the fractionation behaviour after release into MSS suggest that Sec22p, Pma1p and Dpm1p are released into MSS in different forms of vesicles. We hereafter focus our attention on the novel, putative membrane vesicles carrying Dpm1p.

Dpm1p Is Present Not Only In the ER But Also In LDs—Dpm1p, a 30 kD protein possessing one predicted

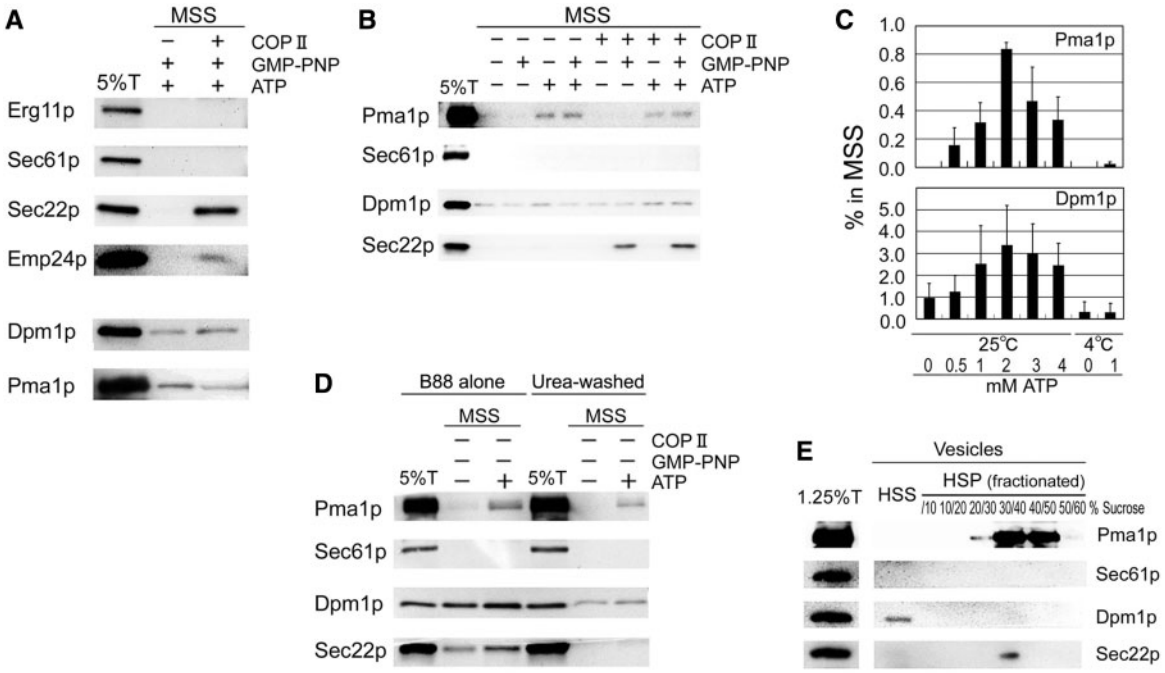

Fig. 1. ***In vitro* budding reactions with yeast microsomes.** Vesicle fractions were analysed by SDS-PAGE followed by immunoblotting with antibodies for various marker proteins. A: Five percent of the total reaction (5%T) and proteins in MSS isolated after incubation at 25°C with (+) or without (−) COPII proteins in the presence of GMP-PNP and 1 mM ATP were analysed. B: *In vitro* budding reactions were performed with or without GMP-PNP, 1 mM ATP and COPII proteins in various combinations at 25°C. C: ATP- and temperature-dependencies of recovery of Pma1p and Dpm1p into MSS. The budding reaction was performed in the presence of various concentrations of ATP at 25 or 4°C. GMP-PNP and COPII proteins were omitted from the reaction mixture. The levels of the proteins in MSS were evaluated on the basis of the 5% total input. Error bars represent SD of three to five independent experiments. D: A comparison of the budding efficiencies from microsomes washed with buffer B88 alone or 2.5 M urea. *In vitro* budding reactions with or without 1 mM ATP were performed in the absence of GMP-PNP and COPII proteins at 25°C. E: Fractionation of vesicles. The MSS obtained from the reaction with GMP-PNP, 1 mM ATP and COPII proteins at 25°C was separated into HSS and HSP. The HSP was loaded on a discontinuous sucrose gradient (10/20/30/40/50/60%, w/w) in 10 mM Hepes-KOH, pH 7.4, and then centrifuged at 166,000g_{av} for 2 h at 4°C. The interfacial fractions, the HSS and 1.25% of the total reaction (1.25% T) were analysed.

transmembrane domain near the C-terminus, is dolichol phosphate mannose synthase, which has been believed to reside in the ER (*39*, *40*). However, a recent proteomic study identified Dpm1p in a purified LD fraction from *S. cerevisiae* cells (*41*). To test the possibility that Dpm1p is indeed in LDs, we examined the intracellular localization of Dpm1p. As shown in Fig. 2A, Dpm1p-GFP exhibits punctate fluorescence in addition to the typical ER pattern. The bright puncta appeared to be in association with the ER, and their positions coincided with light diffractive particles in the Nomarski images, which are characteristic of yeast LDs. RFP fusion of Erg6p, a marker of yeast LDs (*33*), co-localized with Dpm1p-GFP on the puncta (Fig. 2B). Furthermore, Nile Red, a neutral lipid probe used to visualize LDs, stained these puncta of Dpm1p-GFP (Fig. 2C). Figure 2D shows dual colour immunofluorescence microscopy of endogenous Dpm1p and Srt1p-3HA, another LD protein (*42*). Srt1p-3HA also partially co-localized with Dpm1p, and their merge was less frequent than that of Srt1p-3HA and Erg6p-3myc (data not shown).

To examine the distribution of Dpm1p between the ER and LDs, we isolated LDs from cell lysates by the method described under Materials and methods. As shown in Table 1, the prepared LD fraction had very high enrichment of ergosterol and ergosteryl esters over phospholipids as compared to microsomes. We then examined localization of various membrane proteins in this fraction and microsomes. As shown in Fig. 2E, Erg6p-3myc and Srt1-3HA were highly enriched in the LD fraction. Dpm1p-GFP and endogenous Dmp1p were obviously detected in the fraction, whereas other ER proteins, Erg11p and Sec61p were slightly detected. Pma1p, Sed5p (a *cis*-Golgi marker), Tim23p (a mitochondria marker) and Pho8p (a vacuolar marker) were undetectable in the LD fraction, although they were detectable in microsomes, probably due to cross-contaminations of the membranes. The purity of the LDs isolated by our method was considered high (also see Fig. 5A), but they appeared to contain ER components as well.

From these results, we concluded that Dpm1p resides not only in the ER but also in LDs.

The LD Marker Erg6p-3myc Also Bud Into the HSS Fraction—Now the possibility rises that the novel vesicles containing Dpm1p, which we found in the *in vitro* budding reaction, may be the intermediate carrier from the ER to the LDs. So we went back to the assay and examined the behaviour of two more LD proteins, Erg6p-3myc and Srt1p-3HA. Although Erg6p

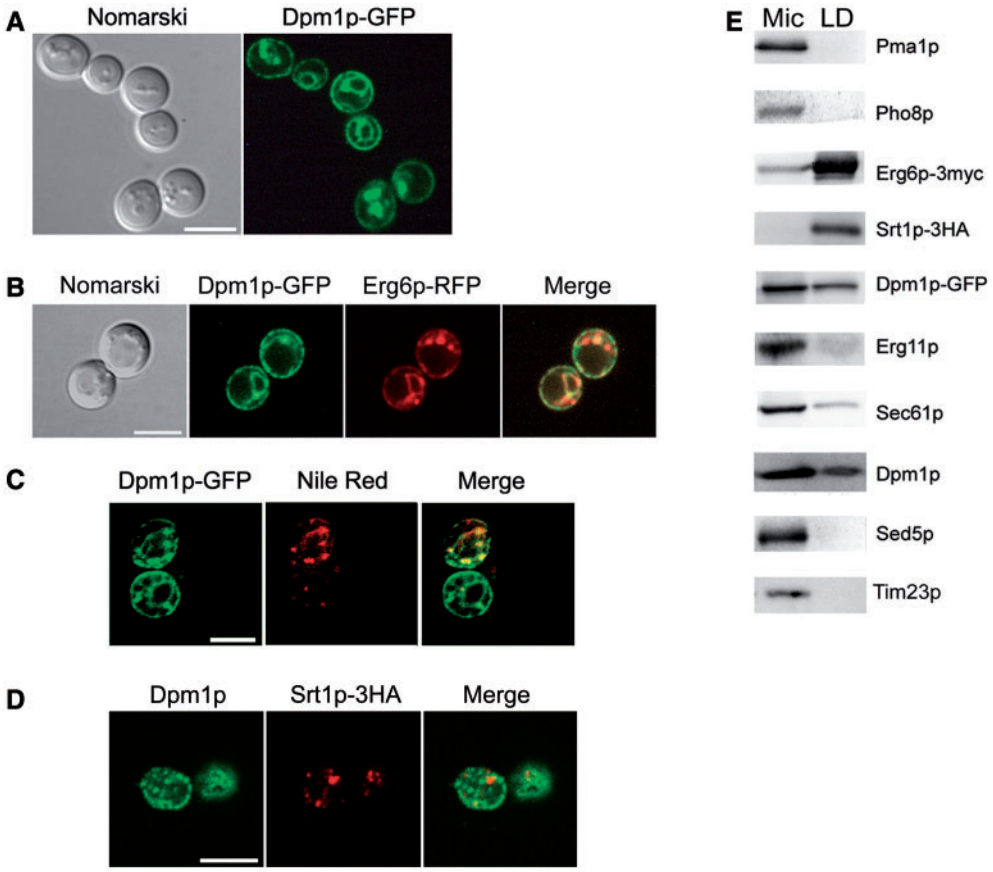

Fig. 2. **Intracellular localization of Dpm1p.** A: Subcellular localization of Dpm1p-GFP. Yeast cells (YPH500) expressing Dpm1p-GFP were observed by confocal microscopy. Nomarski (left panel in the pair) and fluorescence (right panel in the pair) images in the same field are shown. B: Confocal microscopy of yeast cells (KUY136) co-expressing Dpm1p-GFP and Erg6p-RFP. C: Dual colour fluorescence images of Dpm1p-GFP and Nile Red. The cells (YTY102) were stained with Nile Red (final 1 μg/ml) and observed by confocal microscopy. D: Dual colour immunofluorescnece images of endogenous Dpm1p and Srt1p-3HA. Yeast cells (KUY136) co-expressing Srt1p-3HA and Erg6p-3myc were immunostained by anti-Dpm1p and anti-HA (Y-11) antibodies. In A–D, bars = 5 μm. E: Immunoblotting analysis of microsomes and the LD fraction. Fractions were prepared from cells at a late log phase. All protein contents were determined by the method of Peterson (*31*). Five micrograms of protein of microsomes (Mic) and of the LDs were analysed by immunoblotting using antibodies for various markers.

and Srt1p possess no and one predicted transmembrane domain, respectively, neither of them was removed from microsomes after the urea washing (data not shown). As shown in Fig. 3A, Erg6p-3myc and Dpm1p-GFP were clearly recovered in the HSS fraction after the reaction at 25°C, as was endogenous Dpm1p. Srt1p-3HA was detected abundantly in the LD fraction (Fig. 2E) but not in HSS. This suggests that Srt1p may be released from the ER by another distinct pathway, and more importantly, it indicates that the novel vesicles we were observing were not the LDs themselves.

We next examined the effect of the addition of 1 mM glycerol-3-phosphate and 0.1 mM oleoyl-CoA in the assay since LDs contribute to biosynthesis of various lipids including glycerolipids and neutral lipids (*43*). As shown in Fig. 3B, the recovery of Dmp1-GFP, Erg6p-3my as well as endogenous Dpm1p in MSS was all enhanced by the addition of glycerol-3-phosphate and oleoyl-CoA, and the increase was further augmented by the presence of ATP (*lanes* 1–4). Release of Sec61p into MSS was hardly stimulated by these compounds. The addition of oleoyl-CoA and ATP without glycerol-3-phosphate rendered more marked effect (*lanes* 2–6), implying that non-glycerolipids, such as steryl esters, could increase formation of the vesicles. The three proteins were similarly released into the vesicle fraction under the same conditions, and the enhanced release was recovered in HSS (*lane* 7).

Features Of the Novel Vesicles Carrying Dpm1p—Detailed fractionation behaviour of the novel vesicles from non-urea-washed microsomes was investigated to identify why they partitioned into HSS. The distribution of Dpm1p, Erg6p-3myc and Dpm1p-GFP in the centrifugal tube after the centrifugation at 200,000g_{max} for 15 min was examined. As shown in Fig. 4A, all three proteins distributed mostly equally from top to bottom in HSS, although the isolated LDs were floated to the top after the same centrifugation (data not shown). This observation raised the possibilities that the density of the vesicles was nearly equal to that of the solvent ($\rho = 1.032$ g/ml), and/or the vesicles were so small that they were not sedimented/floated by this centrifugation. To elucidate these possibilities, HSS was further centrifuged at 200,000g_{max} for 1 h in the fixed angle rotor

Table 1. **Lipid content of microsomes and the lipid droplet fraction.**

Fraction	Phospholipids:protein (μmol/mg)	Ratio of	
		Ergosterol:phospholipids (mol/mol)	Ergosteryl ester: phospholipids (mol/mol)
Microsomes	0.50 ± 0.09	0.06 ± 0.04	0.15 ± 0.08
Lipid droplets	0.30 ± 0.15	1.13 ± 0.07	4.85 ± 0.63

Means ± SD of three to five different isolations from the cells (YPH500) grown in YPD at the late log phase were shown. Proteins in microsomes were quantified by the methods of Bradford (*30*), and the LDs by Peterson (*31*), respectively.

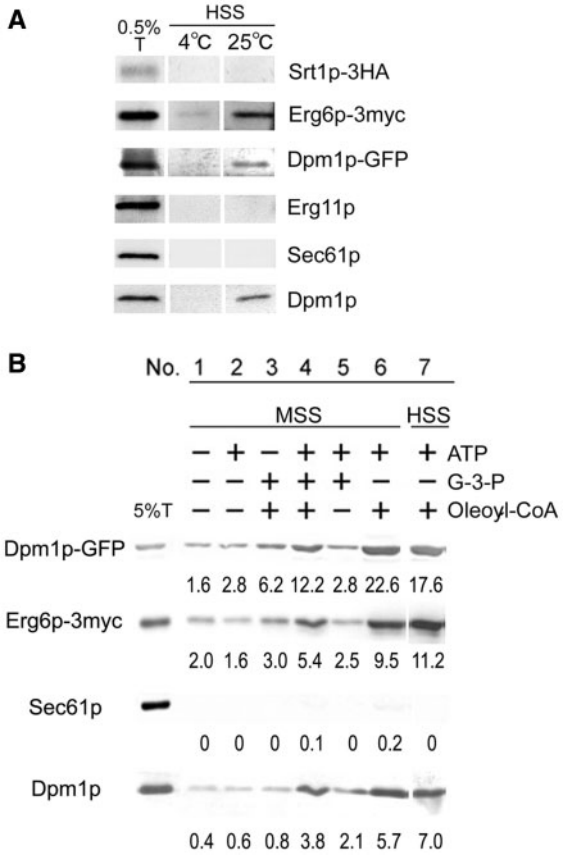

Fig. 3. ***In vitro* budding of lipid droplet proteins.** A: Temperature-dependent recovery of various markers into the HSS fraction in the budding assay. The budding reactions were performed with no additive at 4°C or 25°C. After the reaction and subsequent fractionation, the HSS was analysed together with 0.5% total input (0.5%T) by immunoblotting. B: Effect of substrates supporting lipid biosynthesis on the budding reaction. Microsomes were prepared from the wild-type cells (YPH500) expressing Dpm1p-GFP and Erg6p-3myc. The budding reactions were performed with (+) or without (−) 1 mM ATP, 1 mM glycerol-3-phosphate (G-3-P) and 0.1 mM oleoyl-CoA in various combinations at 25°C. MSS and HSS were obtained and analysed. The budding efficiency of each protein was calculated on the basis of the 5% total input (5%T), and indicated under each band.

and the distribution of the vesicles was examined. After the centrifugation, the three proteins were all recovered in the pellet, while human transferrin, a soluble protein exogenously added into HSS, was not (Fig. 4B), indicating that the vesicles were denser than the solvent. By sucrose-gradient floatation ultracentrifugation, Dpm1p from HSS was floated at around the $\rho = 1.15$–1.19 g/ml fraction, while transferrin remained at the bottom (Fig. 4C). Dpm1p-GFP showed the same fractionation pattern as endogenous Dpm1p, but Erg6p-3myc became undetectable after the floatation centrifugation for unknown reasons (data not shown).

The pelletable membranes in HSS from the cells expressing Dpm1p-GFP after the additional centrifugation (Fig. 4B) were fixed by 4% paraformaldehyde and directly applied to a grid for electron microscopy. They were immunolabeled with anti-GFP antibodies followed by the gold-conjugated second antibodies, stained with uranyl acetate, and then viewed under an electron microscope. As shown in Fig. 4D, highly immunolabeled small vesicles and saccules, most of which were 40–50 nm in diameter, were observed, representing Dpm1p-GFP was present on them. The labeling was scarce and such a labeling was not observed in the absence of anti-GFP antibodies and in the fraction from the cells expressing no GFP-fusion protein (data not shown).

Fluorescence Microscopic Observation Of the Isolated LDs—We also tried to visualize Dmp1p-GFP in the isolated LDs by fluorescence microscopy. Figure 5A shows a Nomarski image and Nile Red staining of the LDs, also confirming the high purity of Nile Red-positive LDs. The isolated LDs were often larger in size than those seen in the cells (around 1 μm in diameter), probably due to homotypic fusion. In the LDs, Dpm1p-GFP often showed punctate fluorescence and non-continuous localization in the LDs (Fig. 5B). In contrast, Erg6p-RFP was observed mostly on the surface in a continuous manner (Fig. 5C).

DISCUSSION

In the present study, we found *in vitro* budding of a novel type of membrane vesicles carrying Dpm1p (Figs. 1, 3 and 4), which are distinct in size, appearance and biochemical characteristics from the three well-characterized transport vesicles, COPII, COPI and clathrin-coated vesicles (*44*). We also confirmed the localization of Dpm1p to LDs as well as to the ER (Fig. 2). The ATP-dependent formation of vesicles carrying Pma1p, a plasma membrane H^+-ATPase, was also found (Fig. 1). Although we did not pursue the latter vesicles, these might be a kind of endocytic vesicles from the plasma membrane contaminating in microsomes since Pma1p is a major plasma membrane protein (*45*).

The experimental results in Fig. 3 suggest that the novel vesicles are precursors/transport vesicles for LDs. The precise mechanism for the formation of the vesicles is unclear, but the content and/or synthesis of several

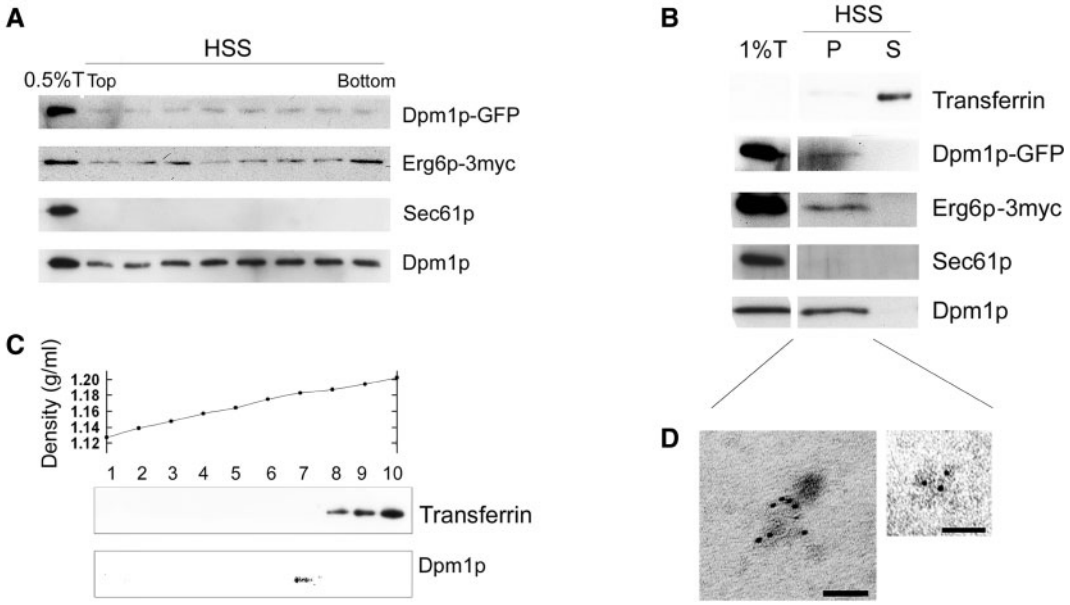

Fig. 4. **Fractionation behaviour and appearance of the novel vesicles.** Non-urea-washed microsomes were used in the budding reactions with no additive at 25°C. A: Distribution of Dpm1p, Dpm1p-GFP and Erg6p-3myc in the HSS fraction. After the ultracentrifugation of MSS for 15 min, eight fractions were taken from top to bottom of HSS. The fractions and the 0.5% total reaction (0.5%T) were analysed by SDS-PAGE and immunoblotting. B: Recovery of the vesicles into the pelletable fraction. HSS was diluted 4-folds with buffer B88, and then further centrifuged at 200,000g_{max} in the TLA120.2 rotor for 1 h. The resulting pellet (P) and supernatant (S) were analysed. C: Flotation of the vesicles. HSS was mixed with two volumes of 60% (w/w) sucrose in Hepes, pH 7.4, and was placed at the bottom of a centrifuge tube. Then layers of 35, 30 and 25% (w/w) sucrose/Hepes were layered on the top. The gradient was centrifuged at 166,000g_{av} for 14.5 h at 4°C. Ten fractions were taken from top to bottom, and analysed. In B and C, human transferrin was included in HSS as a soluble protein marker. D: Immunoelectron microscopy of the pelletable membranes in HSS. The membranes in HSS were pelleted as in B, paraformaldehyde-fixed, and then mounted on a grid. They were immunolabeled with anti-GFP antibodies followed by the second antibodies conjugated with 6 nm gold. Bars = 100 nm.

lipids would be important (Fig. 3B). Although it remains to be determined which lipid can indeed stimulate the vesicle budding, it is intriguing to resolve how lipid biosynthesis and the sorting event of Dpm1p and Erg6p are linked. The reason why Dpm1p also resides in LDs is still unclear. Srt1p, which is preferentially present in LDs, is a *cis*-prenyltransferase also involving in dolichol synthetic pathway (*42*). Therefore, LDs may contribute to biosynthesis of dolichyl lipids in addition to the ER and Dpm1p could be actively sorted and transported to LDs, while Srt1p-3HA was not found in the vesicle fraction (Fig. 3A) and its transport mechanism to LDs remains unknown.

Despite that the vesicles would be the intermediates of LDs, they are not buoyant as the LDs (Fig. 4A–C), probably due to high protein-to-lipid ratio. On the other hand, the vesicles were of fairly small structures (Fig. 4D) and thus remained in the HSS after the centrifugation at 200,000g_{max} for 15 min, and needed a longer time to be sedimented (Figs. 1E, 3, 4A and 4B).

Caveolin-1 containing spherical lipid droplets was reported to derive from microsomes in a mammalian cell-free system (*46*), and the droplets were recovered in the $\rho \leq 1.06$ g/ml fractions after gradient ultracentrifugation and with similar size and appearance to isolated LDs. On the other hand, the novel vesicles we found in the present study, which could also be LD precursors, were recovered in heavier fractions and were morphologically distinct from the isolated LDs. Therefore, we would be observing different phenomena related to LD biogenesis.

In fluorescence microscopy, Dpm1p-GFP was located in confined subregions of the LDs (Fig. 5B). It is suggested that Dpm1p are localized to specific subdomains in LDs, and the novel vesicles found in this study may contribute to make the subdomains in LDs and/or transport LD proteins there. In intact cells, Dpm1p-GFP-negative LDs were also found in the cells (Fig. 2A–D). This observation suggests that the protein compositions of LDs vary even in a single cell.

It is currently accepted that Dpm1p is oriented to the cytoplasmic surface of the ER (*47*), namely, the long soluble peptide in the N-terminal side is exposed to cytoplasm. However, some reports are contradictory as to the orientation of Dpm1p. Immunoelectron microscopy showed that gold-conjugated secondary antibodies that reacted with anti-Dpm1p antibodies raised against the soluble N-terminal peptide were rarely found within the lumenal space of the ER in *S. cerevisiae* cells (*48*). On the other hand, the enzyme activity of Dpm1p was hardly decreased by trypsin-treatment of isolated membranes in the absence of a detergent (*49*). In the present study, Dpm1p-GFP on the paraformaldehyde-fixed novel vesicles could effectively be immunolabeled by anti-GFP antibodies followed by the gold-conjugated second antibodies, despite that the fixed membranes were not permeabilized by any detergent (Fig. 4D). This result

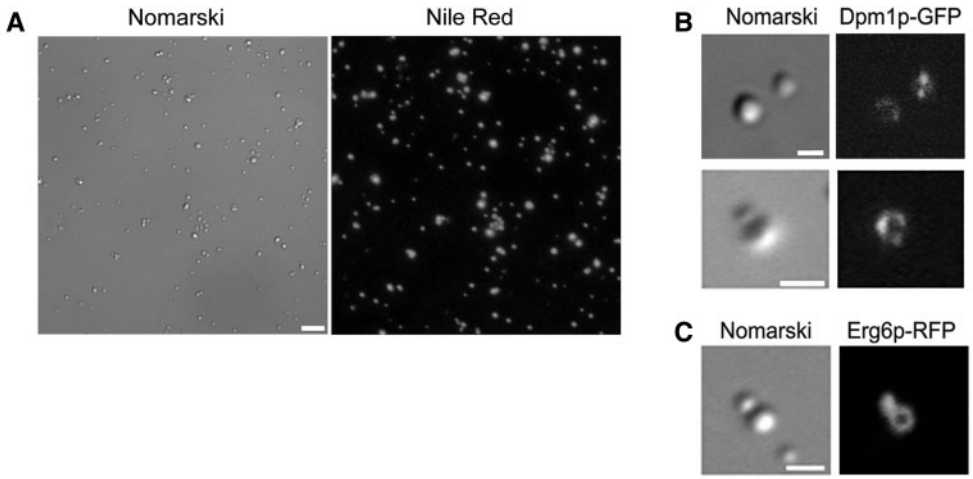

Fig. 5. **Fluorescence microscopic observation of isolated lipid droplets.** A: The LDs isolated from the cells of wild-type strain (YPH500) expressing no fluorescence fusion protein were stained with Nile Red, and then observed by fluorescence microscopy. Bar = 5 μm. B and C: Fluorescence images of the LDs from the YPH500 strain expressing Dpm1p-GFP (B) and the KUY136 strain expressing Erg6p-RFP (C). Bars = 1 μm.

suggests that the C-terminus of Dpm1p-GFP is exposed on the cytoplasmic surface, and accordingly the N-terminal peptide may face the lumen. Our result of *in vitro* protease assay utilizing microsomes and anti-Dpm1p antibodies favours the lumenal orientation of Dpm1p (our unpublished data). The topology of Dpm1p and Dpm1p-GFP in LDs also remains to be elucidated. More systematic experiments will be required to confirm the transmembrane topology of Dpm1p in these membranes.

It has long been considered that LDs are formed by a simple budding mechanism (*1–4*). However, Robenek *et al*. (*50*) reported that LDs could grow in a close position to the ER, not within the ER membranes. In addition, the precursors/transport vesicles for LDs we found were considerably small. The model for the LD formation would need to be corrected. To understand the complicated and elaborate mechanisms of the LD formation, more detailed biochemical and morphological analysis of the novel vesicles as well as LDs will be necessary.

We are grateful to Randy Schekman (University of California, Berkeley, CA), Toshiya Endo (Nagoya University), Ryogo Hirata and Coichi Nihei (RIKEN) for antibodies. We also thank Takashi Ueda (University of Tokyo) for kind help in the use of LSM-510, Kumi Matsuura-Tokita (RIKEN) for plasmids, and the members of the Nakano laboratory for fruitful discussions. Yuichi Takeda was a Special Postdoctoral Researcher of RIKEN.

REFERENCES

1. Murphy, D.J. and Vance, J. (1999) Mechanisms of lipid-body formation. *Trends Biochem. Sci.* **24**, 109–115
2. Zweytick, D., Athenstaedt, K., and Daum, G. (2000) Intracellular lipid particles of eukaryotic cells. *Biochim. Biophys. Acta* **1469**, 101–120
3. Brown, D.A. (2001) Lipid droplets: proteins floating on a pool of fat. *Curr. Biol.* **11**, R446–R449
4. Murphy, D.J. (2001) The biogenesis and functions of lipid bodies in animals, plants and microorganisms. *Prog. Lipid Res.* **40**, 325–438
5. Tauchi-Sato, K., Ozeki, S., Houjou, T., Taguchi, R., and Fujimoto, T. (2002) The surface of lipid droplets is a phospholipid monolayer with a unique fatty acid composition. *J. Biol. Chem.* **277**, 44507–44512
6. Martin, S. and Parton, R.G. (2006) Lipid droplets: a unified view of a dynamic organelle. *Nat. Rev. Mol. Cell Biol.* **7**, 373–378
7. Brasaemle, D.L., Dolios, G., Shapiro, L., and Wang, R. (2004) Proteomic analysis of proteins associated with lipid droplets of basal and lipolytically stimulated 3T3-L1 adipocytes. *J. Biol. Chem.* **279**, 46835–46842
8. Liu, P., Ying, Y., Zhao, Y., Mundy, D.I., Zhu, M., and Anderson, R.G. (2004) Chinese hamster ovary K2 cell lipid droplets appear to be metabolic organelles involved in membrane traffic. *J. Biol. Chem.* **279**, 3787–3792
9. Umlauf, E., Csaszar, E., Moertelmaier, M., Schuetz, G.J., Parton, R.G., and Prohaska, R. (2004) Association of stomatin with lipid bodies. *J. Biol. Chem.* **279**, 23699–23709
10. Sato, S., Fukasawa, M., Yamakawa, Y., Natsume, T., Suzuki, T., Shoji, I., Aizaki, H., Miyamura, T., and Nishijima, M. (2006) Proteomic profiling of lipid droplet proteins in hepatoma cell lines expressing hepatitis C virus core protein. *J. Biochem. (Tokyo)* **139**, 921–930
11. Andersson, L., Boström, P., Ericson, J., Rutberg, M., Magnusson, B., Marchesan, D., Ruiz, M., Asp, L., Huang, P., Frohman, M.A., Borén, J., and Olofsson, S.O. (2006) PLD1 and ERK2 regulate cytosolic lipid droplet formation. *J. Cell Sci.* **119**, 2246–2257
12. Funato, K. and Riezman, H. (2001) Vesicular and nonvesicular transport of ceramide from ER to the Golgi apparatus in yeast. *J. Cell Biol.* **155**, 949–959
13. Barlowe, C., Orci, L., Yeung, T., Hosobuchi, M., Hamamoto, S., Salama, N., Rexach, M.F., Ravazzola, M., Amherdt, M., and Schekman, R. (1994) COPII: a membrane coat formed by Sec proteins that drive vesicle budding from the endoplasmic reticulum. *Cell* **77**, 895–907
14. Nakano, A. and Muramatsu, M. (1989) A novel GTP-binding protein, Sar1p, is involved in transport from the endoplasmic reticulum to the Golgi apparatus. *J. Cell Biol.* **109**, 2677–2691
15. Kuehn, M.J., Herrmann, J.M., and Schekman, R. (1998) COPII-cargo interactions direct protein sorting into ER-derived transport vesicles. *Nature* **391**, 187–190
16. Kuehn, M.J., Schekman, R., and Ljungdahl, P.O. (1996) Amino acid permeases require COPII components and the

ER resident membrane protein Shr3p for packaging into transport vesicles *in vitro*. *J. Cell Biol.* **135**, 585–595
17. Otte, S., Belden, W.J., Heidtman, M., Liu, J., Jensen, O.N., and Barlowe, C. (2001) Erv41p and Erv46p: new components of COPII vesicles involved in transport between the ER and Golgi complex. *J. Cell Biol.* **152**, 503–518
18. Sato, K. and Nakano, A. (2002) Emp47p and its close homolog Emp46p have a tyrosine-containing endoplasmic reticulum exit signal and function in glycoprotein secretion in *Saccharomyces cerevisiae*. *Mol. Biol. Cell* **13**, 2518–2532
19. Supek, F., Madden, D.T., Hamamoto, S., Orci, L., and Schekman, R. (2002) Sec16p potentiates the action of COPII proteins to bud transport vesicles. *J. Cell Biol.* **158**, 1029–1038
20. Sikorski, R.S. and Hieter, P. (1989) A system of shuttle vectors and yeast host strains designed for efficient manipulation of DNA in *Saccharomyces cerevisiae*. *Genetics* **122**, 19–27
21. Umebayashi, K. and Nakano, A. (2003) Ergosterol is required for targeting of tryptophan permease to the yeast plasma membrane. *J. Cell Biol.* **161**, 1117–1131
22. Ueda, T., Matsuda, N., Anai, T., Tsukaya, H., Uchimiya, H., and Nakano, A. (1996) An Arabidopsis gene isolated by a novel method for detecting genetic interaction in yeast encodes the GDP dissociation inhibitor of Ara4 GTPase. *Plant Cell* **8**, 2079–2091
23. Takeuchi, M., Tada, M., Saito, C., Yashiroda, H., and Nakano, A. (1998) Isolation of a tobacco cDNA encoding Sar1 GTPase and analysis of its dominant mutations in vesicular traffic using a yeast complementation system. *Plant Cell Physiol.* **39**, 590–599
24. Schimmöller, F., Singer-Krüger, B., Schröder, S., Krüger, U., Barlowe, C. and Riezman, H. (1995) The absence of Emp24p, a component of ER-derived COPII-coated vesicles, causes a defect in transport of selected proteins to the Golgi. *EMBO J.* **14**, 1329–1339
25. Bednarek, S.Y., Ravazzola, M., Hosobuchi, M., Amherdt, M., Perrelet, A., Schekman, R., and Orci, L. (1995) COPI- and COPII-coated vesicles bud directly from the endoplasmic reticulum in yeast. *Cell* **83**, 1183–1196
26. Stirling, C.J., Rothblatt, J., Hosobuchi, M., Deshaies, R., and Schekman, R. (1992) Protein translocation mutants defective in the insertion of integral membrane proteins into the endoplasmic reticulum. *Mol. Biol. Cell* **3**, 129–142
27. Sato, K. and Nakano, A. (2003) Oligomerization of a cargo receptor directs protein sorting into COPII-coated transport vesicles. *Mol. Biol. Cell* **14**, 3055–3063
28. Homma, K., Yoshida, Y., and Nakano, A. (2000) Evidence for recycling of cytochrome P450 sterol 14-demethylase from the cis-Golgi compartment to the endoplasmic reticulum (ER) upon saturation of the ER-retention mechanism. *J. Biochem. (Tokyo)* **127**, 747–754
29. Wuestehube, L.J. and Schekman, R.W. (1992) Reconstitution of transport from endoplasmic reticulum to Golgi complex using endoplasmic reticulum-enriched membrane fraction from yeast. *Methods Enzymol.* **219**, 124–136
30. Bradford, M.M. (1976) A rapid and sensitive method for the quantitation of microgram quantities of protein utilizing the principle of protein-dye binding. *Anal. Biochem.* **72**, 248–254
31. Peterson, G.L. (1977) A simplification of the protein assay method of Lowry et al. which is more generally applicable. *Anal. Biochem.* **83**, 346–356
32. Leber, R., Landl, K., Zinser, E., Ahorn, H., Spök, A., Kohlwein, S.D., Turnowsky, F., and Daum, G. (1998) Dual localization of squalene epoxidase, Erg1p, in yeast reflects a relationship between the endoplasmic reticulum and lipid particles. *Mol. Biol. Cell* **9**, 375–386
33. Athenstaedt, K., Zweytick, D., Jandrositz, A., Kohlwein, S.D., and Daum, G. (1999) Identification and characterization of major lipid particle proteins of the yeast Saccharomyces cerevisiae. *J. Bacteriol.* **181**, 6441–6448
34. Russell, S.J., Steger, K.A., and Johnston, S.A. (1999) Subcellular localization, stoichiometry, and protein levels of 26 S proteasome subunits in yeast. *J. Biol. Chem.* **274**, 21943–21952
35. Folch, J., Lees, M., and Sloane Stanley, G.H. (1957) A simple method for the isolation and purification of total lipides from animal tissues. *J. Biol. Chem.* **226**, 497–509
36. Rouser, G., Fkeischer, S., and Yamamoto, A. (1970) Two dimensional then layer chromatographic separation of polar lipids and determination of phospholipids by phosphorus analysis of spots. *Lipids* **5**, 494–496
37. Shaw, W.H.C. and Jefferies, J.P. (1953) The determination of ergosterol in yeast. *The Analyst* **78**, 509–514
38. Martin, S., Tellam, J., Livingstone, C., Slot, J.W., Gould, G.W., and James, D.E. (1996) The glucose transporter (GLUT-4) and vesicle-associated membrane protein-2 (VAMP-2) are segregated from recycling endosomes in insulin-sensitive cells. *J. Cell Biol.* **134**, 625–635
39. Orlean, P., Albright, C., and Robbins, P.W. (1988) Cloning and sequencing of the yeast gene for dolichol phosphate mannose synthase, an essential protein. *J. Biol. Chem.* **263**, 17499–17507
40. Orlean, P. (1990) Dolichol phosphate mannose synthase is required *in vivo* for glycosyl phosphatidylinositol membrane anchoring, O mannosylation, and N glycosylation of protein in *Saccharomyces cerevisiae*. *Mol. Cell. Biol.* **10**, 5796–5805
41. Binns, D., Januszewski, T., Chen, Y., Hill, J., Markin, V.S., Zhao, Y., Gilpin, C., Chapman, K.D., Anderson, R.G., and Goodman, J.M. (2006) An intimate collaboration between peroxisomes and lipid bodies. *J. Cell Biol.* **173**, 719–731
42. Sato, M., Fujisaki, S., Sato, K., Nishimura, Y., and Nakano, A. (2001) Yeast *Saccharomyces cerevisiae* has two *cis*-prenyltransferases with different properties and localizations. Implication for their distinct physiological roles in dolichol synthesis. *Genes Cells* **6**, 495–506
43. Daum, G., Lees, N.D., Bard, M., and Dickson, R. (1998) Biochemistry, cell biology and molecular biology of lipids of *Saccharomyces cerevisiae*. *Yeast* **14**, 1471–1510
44. Kirchhausen, T. (2000) Three ways to make a vesicle. *Nat. Rev. Mol. Cell Biol.* **1**, 187–198
45. Morsomme, P., Slayman, C.W., and Goffeau, A. (2000) Mutagenic study of the structure, function and biogenesis of the yeast plasma membrane H(+)-ATPase. *Biochim. Biophys. Acta* **1469**, 133–157
46. Marchesan, D., Rutberg, M., Andersson, L., Asp, L., Larsson, T., Borén, J., Johansson, B.R., and Olofsson, S.O. (2003) A phospholipase D-dependent process forms lipid droplets containing caveolin, adipocyte differentiation-related protein, and vimentin in a cell-free system. *J. Biol. Chem.* **278**, 27293–27300
47. Herscovics, A. and Orlean, P. (1993) Glycoprotein biosynthesis in yeast. *FASEB J.* **7**, 540–550
48. Preuss, D., Mulholland, J., Kaiser, C.A., Orlean, P., Albright, C., Rose, M.D., Robbins, P.W., and Botstein, D. (1991) Structure of the yeast endoplasmic reticulum: localization of ER proteins using immunofluorescence and immunoelectron microscopy. *Yeast* **7**, 891–911
49. Haselbeck, A. (1989) Purification of GDP mannose: dolichyl-phosphate O-beta-D-mannosyltransferase from *Saccharomyces cerevisiae*. *Eur. J. Biochem.* **181**, 663–668
50. Robenek, H., Hofnagel, O., Buers, I., Robenek, M.J., Troyer, D., and Severs, N.J. (2006) Adipophilin-enriched domains in the ER membrane are sites of lipid droplet biogenesis. *J. Cell Sci.* **119**, 4215–4224